SAND-WATER SLURRY FLOW MODELLING IN A HORIZONTAL PIPELINE BY COMPUTATIONAL FLUID DYNAMICS TECHNIQUE

Tamer Nabil [1], Imam El-Sawaf[2], and Kamal El-Nahhas[3]

[1]Assistant lecturer, Faculty of Engineering, Suez Canal University, Ismailia, Egypt
E-mail: tamer_mtc@yahoo.com
[2]Professor, Faculty of Engineering, Port Said University, Port Said, Egypt
E-mail: iaelsawf@hotmail.com
[3] Suez Canal Authority, Egypt, E-mail: k_elnahhas@yahoo.com

ABSTRACT

In this paper,a computational fluid dynamics simulation technique (CFD) is introduced to obtain the numerical solution of sand–water slurry flowand to have better insight about the complexity of slurry flow in pipelines. The model is utilized to predict the concentration profile, velocity profile and their effect on pressure drop, taking the effect of particle size into consideration. At first a two-dimensional model has been developed, then, a three-dimensional model has been generated in order to complete the understanding and visualization of slurry flow behavior. The two-fluid model based on the Eulerian-Eulerian approach along with a standard k-ε turbulence model with mixture properties was used. The Eulerian model is the most complex and computationally intensive among the multiphase models. In particular, it solves a set of momentum and continuity equations for each phase.The computational model was mapped onto the(CFD) solver FLUENT 6.3. The experimental data comprised water-sand slurry with three different particle sizes (0.2, 0.7 and 1.4 mm) at different concentrations (from 5% to 30% by volume) within a wide range of flow velocities (from 0.5 to 5 m/s). In order to evaluate the extent and to push the envelope of applicability of the simulation model, it has been compared with experimental data of the pressure gradient.The model was firstly validated with pressure gradient data of the authors' experiments, and then validated with concentration and velocity profilesfrom the experimental data available in theopen literature. Results of this work show that there is asatisfactory agreement between calculated results and experimental data, especially for fine slurries.

Keywords:CFD,Slurry flow,Concentration and velocity profiles,Pressure drop.
Received June,2013. Accepted March,2014

1. INTRODUCTION

Transportation of slurries through pipeline is common in many industries including foods, pharmaceuticals, chemicalsand miningindustries. It has been aserious concern forresearchers around the world to develop accurate models for pressure drop, velocity profile, and concentration distribution in a slurry pipeline. Efforts done over the years have been enormous,in order to give a better selection of slurry pumps and optimization of power consumption (Wilson et al. [2]). Most of the equations available in previous studies for predicting vertical solids concentration profiles in a slurry pipeline are empirical in nature and have been developed based on limited data for materials having very low concentrations. Much larger concentrations are now coming into common use, showing a more complicated behavior. Concentration distribution may be used to determine the parameters of direct importance (mixture and solid flow rates), flow regime and secondary effects such as wall abrasion and particle degradation.

For higher values of solid concentration, very few experimental data on local concentration are available because of the difficulties in the measurement techniques(Gillies et al. [6]). Considering this, it would be most useful to develop computational models, which will allow a prior estimation of the solid concentration profile and velocity profile over the pipe cross section. In recent years, CFD became a powerful tool, being used in the area like fluid flow relating phenomena by solving mathematical equations that govern these processes using a numerical algorithm on a computer.

In spite of the major difficulties, attempts have been made to simulate the solid-liquid flow in pipelines. The aim is to explore the capability of CFD to model such complex flow. In the present work, the solid suspension in a fully developed pipe flow was simulated. This work presents the usage of atwo-fluid model based on the Eulerian-Eulerian approach, along with a standard k- ε turbulence model with mixture properties.

2. SOLID-LIQUID SLURRY FLOW CFD MODEL

The Eulerian–Eulerian two-fluid model was adopted here. In fact, the Eulerian approach has been reported to be efficient for simulating multiphase flows once the interaction terms are included. The turbulent flow of sand particles in a Newtonian fluid is assumed to be governed by the equations discussed in this section, which form the basis of the Eulerian–Eulerian CFD model used.

2.1 Eulerian Model

For the present CFD simulation, the Eulerian-Eulerian multiphase model implemented in the commercial code Fluent 6.3 was used. With this approach, the continuity and the momentum equations are solved for each phase and therefore, the determination of separate flow field solutions is allowed. The Eulerian model is the most complex and computationally intensive among the multiphase models. It solves a set of 'n' momentum and continuity equations for each phase. Coupling is achieved through the pressure and interphase exchange coefficients. For granular flows, the properties are obtained from the application of kinetic theory, Anderson [1].

2.1.1Continuity Equation

The solution of the continuityequation for each secondary phase, along with the condition that the volume fractions sum to one, allows for the calculation of the primary-phase volume fraction.
The continuity equation for a phase (q) is given by:

$$\frac{\partial}{\partial t}(\alpha_q \rho_q)+\nabla(\alpha_q \rho_q v_q)=0 \tag{1}$$

2.1.2 Momentum Equations

• ***Fluid-fluid momentum equations***
The conservation of momentum (Kaushal et al. [9]) for a fluid phase (q) is:

$$\begin{aligned}\frac{\partial}{\partial t}(\alpha_q \rho_q \overrightarrow{v_q}) + \nabla.(\alpha_q \rho_q \overrightarrow{v_q}\overrightarrow{v_q}) &= -\alpha_q \nabla p - \nabla.\overline{\overline{\tau_q}} + \alpha_q \rho_q \vec{g} \\ &+ \alpha_q \rho_q (\overrightarrow{F_q} + \overrightarrow{F_{lift,q}} + \overrightarrow{F_{Vm,q}}) \\ &+ \sum_{p=1}^{n} (K_{pq}(\overrightarrow{v_p} - \overrightarrow{v_q}) + \dot{m}_{pq}\overrightarrow{v_{pq}})\end{aligned} \tag{2}$$

$$\overline{\overline{\tau_q}} = \alpha_q \mu_q \left(\nabla \vec{v}_q + (\nabla \vec{v}_q)^T\right) + \alpha_q \left(\lambda_q - \frac{2}{3}\mu_q\right)\nabla.\vec{v}_q \bar{\bar{I}} \tag{3}$$

• ***Fluid-solid momentum equation***

The conservation of momentum for the S^{th} solid phase is:

$$\frac{\partial}{\partial t}(\alpha_s \rho_s \overrightarrow{v_s}) + \nabla.(\alpha_s \rho_s \overrightarrow{v_s}\overrightarrow{v_s}) = -\alpha_s \nabla p - \nabla p_s + \nabla.\overline{\overline{\tau_s}} + \alpha_s \rho_s \vec{g} + \alpha_s \rho_s \left(\overrightarrow{F_s} + \overrightarrow{F_{lift,s}} + \overrightarrow{F_{Vm,s}}\right) + \sum_{l=1}^{N} (K_{ls}(\overrightarrow{v_l} - \overrightarrow{v_s}) + \dot{m}_{ls}\overrightarrow{v_{ls}}) \quad (4)$$

where $\dot{m}_{pq}$, $\dot{m}_{ls}$ characterizethe mass transfer rate per unit volume between phases. From the mass conservation $\dot{m}_{pq} = -\dot{m}_{qp}$, $\dot{m}_{ls} = -\dot{m}_{sl}$, $\dot{m}_{pp} = 0$ and $\dot{m}_{ss} = 0$.

• ***Fluid-solid exchange coefficient***

The fluid-solid exchange coefficient K_{sl} is in the following general form;

$$K_{sl} = \frac{\alpha_s \rho_s f}{\tau_s} \quad (5)$$

$$\tau_s = \frac{\rho_s d_s^2}{18\mu_l} \quad (6)$$

wheref is defined differently for the different exchange-coefficient models. All definitions of f include a drag function (C_D) that is based on the relative Reynolds number (Re_s). It is the drag function that differs among the exchange coefficient models. Three models are widely used for calculating solid-liquid interaction:Wen and Yu model, Syamlal-O'Brien model and Gidaspow model.

• ***Solid-solid exchange coefficient***

The solid-solid exchange coefficient K_{ls} has the following form:

$$K_{ls} = \frac{3(1+e_{ls})\left(\frac{\pi}{2} + C_{fr,ls}\frac{\pi^2}{8}\right)\alpha_s \rho_s \alpha_l \rho_l (d_l + d_s)^2 g_{o,ls}}{2\pi\left(\rho_l d_l^3 + \rho_s d_s^3\right)} |\overrightarrow{v_l} - \overrightarrow{v_s}| \quad (7)$$

2.1.3 Solids Shear Stresses

The stress tensor of solids contains shear and bulk viscosities arising from particle momentum exchange due to translation and collision(Liangyong et al. [10]). The collision and kinetic parts, and the optional frictional part, are added to give the solids shear viscosity:

$$\mu_s = \mu_{s,col} + \mu_{s,kin} - \mu_{s,fr} \quad (8)$$

$$\mu_{s,col} = \frac{4}{5}\alpha_s \rho_s d_s g_{o,ss}(1+e_{ss})\left(\frac{\theta_s}{\pi}\right)^{0.5} \quad (9)$$

$$\mu_{s,kin} = \frac{\alpha_s d_s \rho_s \sqrt{\pi\theta_s}}{6(3-e_{ss})}\left(1 + \frac{2}{5}(1+e_{ss})(3e_{ss}-1)\alpha_s g_{o,ss}\right) \quad (10)$$

$$\mu_{s,fr} = \frac{p_s \sin\Phi}{2\sqrt{I_{2D}}} \quad (11)$$

2.2 Turbulent Model

In this study, the simple k-ε turbulence model was assumed. The two phases are assumed to share the same k and ε values and therefore the interphase turbulence transfer is not considered. The k and ε equations describing this model are:

$$\frac{\partial}{\partial t}(\rho_m k) + \nabla.(\rho_m \overrightarrow{v_m} k) = \nabla.\left(\frac{\mu_{t,m}}{\sigma_k}\nabla k\right) + G_{k,m} - \rho_m \varepsilon \quad (12)$$

$$\frac{\partial}{\partial t}(\rho_m \varepsilon) + \nabla.(\rho_m \overrightarrow{v_m} \varepsilon) = \nabla.\left(\frac{\mu_{t,m}}{\sigma_\varepsilon}\nabla \varepsilon\right) + \frac{\varepsilon}{k}\left(C_{1\varepsilon} G_{k,m} - C_{2\varepsilon}\rho_m \varepsilon\right) \quad (13)$$

3. DESCRIPTION OF THE TWO DIMENSIONAL CFD SIMULATION

Initially, the simulation was setup in two dimensions. "Gambit" is one of the softwares in which the geometry can be setup and meshes can be generated. Rectangular pipe geometry (same pipe dimension as in the experiment) wascreated.The pipe length, L, was much higherthan the maximum entrance length, Le, required for a fully developed flow (L/D>200). The geometry was meshed into approximately 1.5×10^5 tetrahedral cells.For Eulerian slurry calculations, we use the Phase Coupled SIMPLE (PC-SIMPLE) algorithm, for the pressure-velocity coupling.Simulations of the carrier fluid flowing alone were performed first, to serve both as an initial validation of the code and the numerical grid, and to reveal the effects of solid particles on the liquid velocity (by deselecting the volume fraction equations). Once the initial solution for the primary phase was obtained, the volume fraction equations were turned back on and the calculation continued with all the phases present.

The first-order upwind discretization scheme was used for the volume fraction, momentum equations, turbulence kinetic energy (k), and turbulence dissipation rate (ε). All the simulations were performed in double numerical precision. Mean velocity as an inletboundary condition and pressure as an outlet boundary conditionwereimposed at the inlet and outlet of the slurry pipeline. The homogeneous volumetric fraction of each phase was specified at the inlet. The usual no-slip boundary condition was adopted at the pipe wall. To avoid divergence, under-relaxation technique was applied. The solution was assumed to have converged when the mass and momentum residuals reached 10^{-4} for all of the solved equations.

4. EXPERIMENTAL SETUP AND MEASURING FACILITIES

An open-loop recirculation pipeline system, shown schematically in Figure (1), was employed for testing the slurry flow behavior (hydraulic resistance curves, Figures 14, 15 and 16). A stainless steel pipe loop of internal diameter 26.8mm was used for slurry parameters measurement (pressure drop). The test section is located in the back (downstream) branch of the piping loop system. A transparent section was mounted at the end of the test section. Pressure measurements were obtained over two sections of the pipe. The pressure is transmitted from the tapping points to three pressure transducersthrough transmission lines and transparent Perspexsedimentation vessels filled with pure water. The control and calibration unit is used to calibrate the sensitive pressure transducers, control different passes to let the transducers read the pressure of any test point and to protect the pump.Pressure transducers were used to measure the pressure losses between the pressure taps. The output signalsof the transducers, which are proportional to the applied pressure, weredisplayed as an analogue value (in milli-ampere). Also these analogue signals were converted into digital signals by adata acquisition system.The digital data were entered in a computer, which is equippedwith the LABVIEW software,enabling online measurement, analysis and storage of the data.

At the downstream end of the test pipes a box divider was mounted,allowing thedischarge to be diverted to a plastic container. Since the divider arm was connected to an electric stopwatch, the mass flow rate wasmeasured,the slurry density and hence the volumetric concentration could be determined. Three sorts of the mono-disperse quartz sands, ρ_s=2650kg/m^3, were used for preparing slurries of the experiments; fine (d_{50}=0.2mm), medium (d_{50}=0.7mm) and coarse (d_{50}=1.4mm). The volumetric concentrations of solids ranged from C_v=5% to 30%.

Due to unavailable feasibility the experimental data of the concentration distributions and velocity profile werecollected from literature, Matousek et al. [5] and Gillies [4], for sand water flow system.

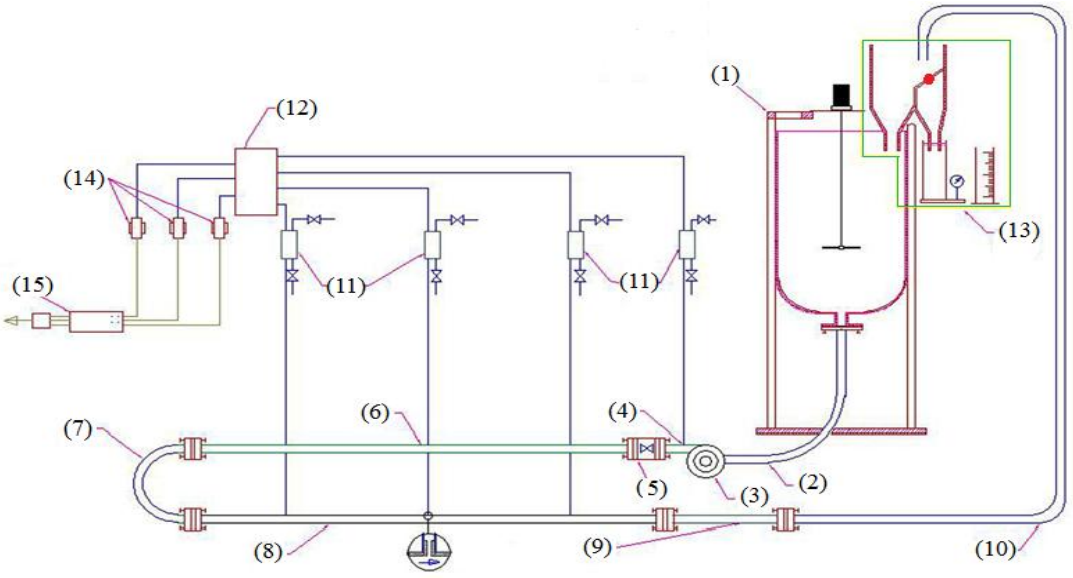

1.Tank with mixer
2.Suction hose
3.Pump
4. Pipeline section (1)
5.Discharge valve
6.Pipeline section (2)
7.Pipeline section (3)
8.Test section
9.Transparent pipe
10.Return hose
11.Sedimentation vessels
12.Control and calibration
13.Flow measuring system
14.Pressure transducers
15. Data acquisition

Fig. 1Schematic diagram of the experimental pipeline test loop

The standard errors (deviations between the mean of measured values and the true value) due to limitations of the measurement equipment or improper calibration, sometimes called “bias”, must be estimated to be ±2.5%. The agreement between the experimental and calculated pressure drop was estimated by the correlation coefficient, which varies according to the solid concentration, slurry velocity and particle size but in all cases didn't exceed 0.1. Correlation coefficient will be unity if the experimental and predicted results perfectly overlap each other.

5. RESULTS AND DISCUSSION OF SIMULATION

5.1 Velocity Profile

Figures 2-7 show the corresponding calculated and experimental vertical velocity profile across the pipe cross section at pipe outlet at different particle diameters, solid concentrations and mean slurry velocities(Liangyong et al. [10]). The velocity profile of the solid phase is generally asymmetrical about the central axis. The asymmetry in the solid phase velocity profile is a result of particle settling due to the density difference between the two phases and the gravitational force effect. The asymmetrical nature of the velocity profile is reduced at higher velocity ranges (say 3-5m/s), with the same concentration and particle size. Also the asymmetrical nature of the velocity profile is reduced at smaller particle size with the same concentration and velocity profile.

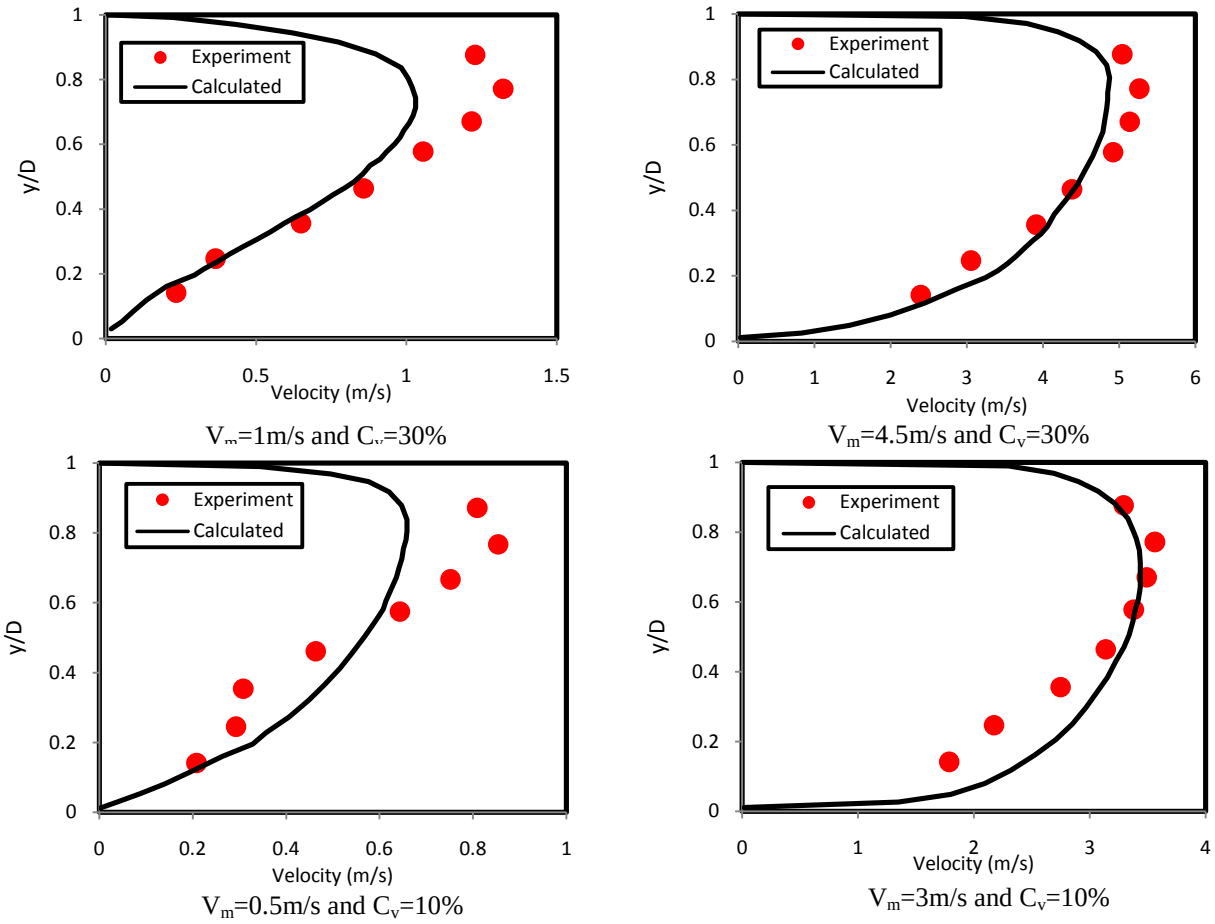

Fig. 2 Vertical velocity profile for flow of 1.4mm sand particle at different concentration and flow velocity

A remarkabledifference of velocity profiles in the figures discussed here, shows that with the increase of solid concentration at the same slurry velocity of the same particle diameter, the asymmetrical nature of velocity profile increases and the position of the maximum velocity moves toward the top half of the pipe; this effect is clearly shown for medium slurry, Figure 5, and relatively for coarse slurry, Figure 3. Figure 7 shows the comparison of velocity profiles at different efflux concentrations at slurry flow velocity of 5m/s for 0.2 mm particles. From this figure, it can be concluded that the velocity profiles for fine particle slurries have a comparatively small changevs. the increase in concentration from 10% to 30%.There's anagreement between experimental and calculated velocity profiles. Suchagreement is very good for fine and medium sand slurries.

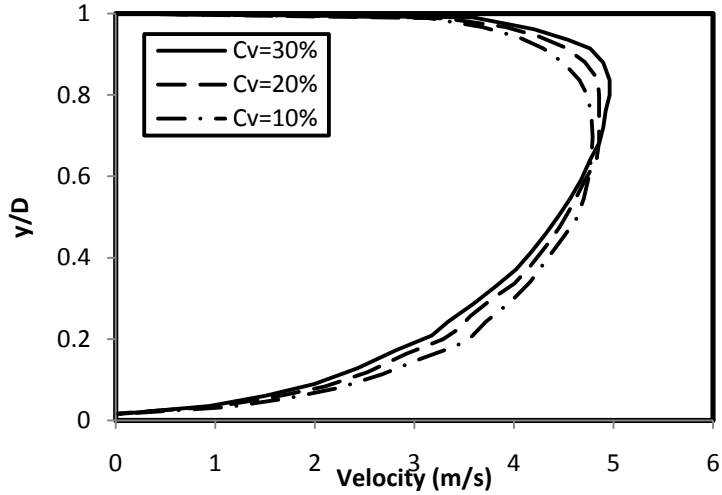

Fig. 3 Vertical velocity profile for flow of 1.4mmsand particle at flow velocity V_m=4m/s and different efflux concentrations

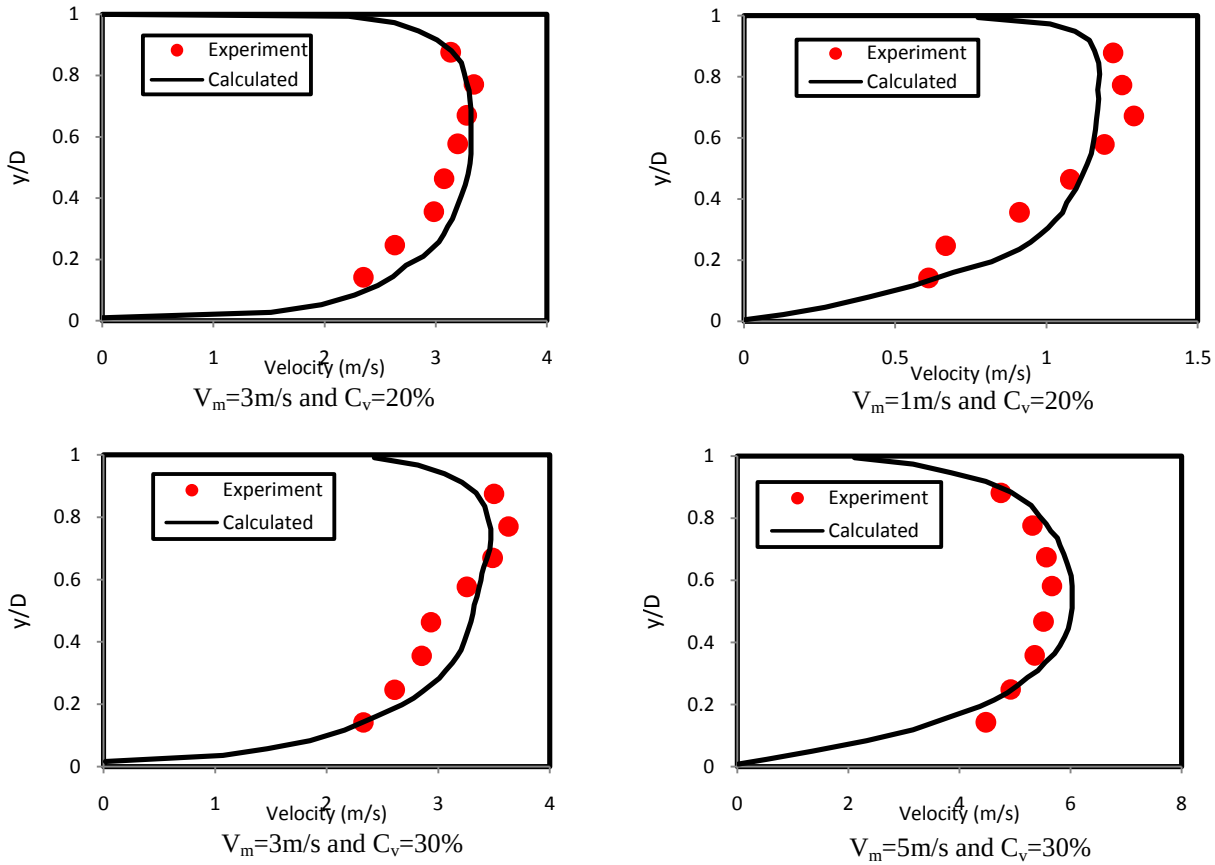

Fig. 4 Vertical velocity profile for flow of 0.7mm sand particle at different concentration and flow velocity

From these figures, it is clear that the slurry mean velocities near the wall drop down sharply due to the strong viscous shear stress in the turbulent boundary layer and non-slip boundary condition(Wilson et al. [14]). The velocity profiles in the lower half of the pipe centerline would be lower than those in the upper half. This occurs because the shear force and the slurry density in the lower part of pipe centerline should be higher than those in the upper part. As a result, water will spend more energy to drive sand particles in the lower part, which results in a lower slurry velocity in this area.

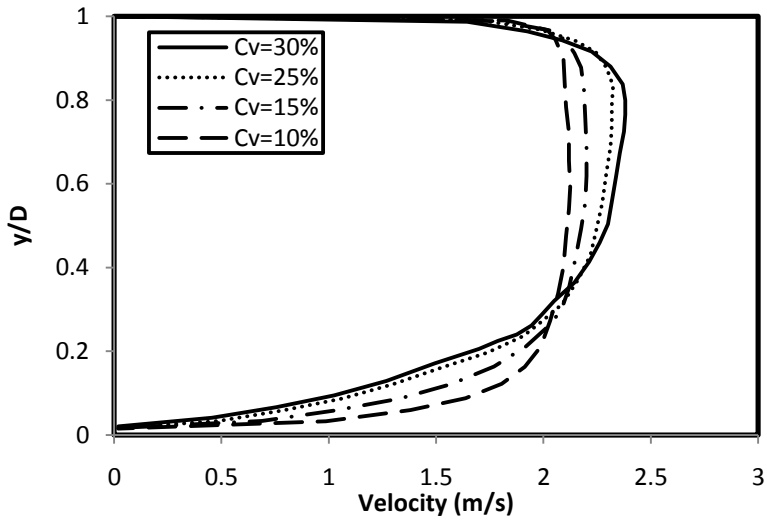

Fig. 5 Vertical velocity profile for flow of 0.7mm particle at velocity V_m=2m/s and different concentrations

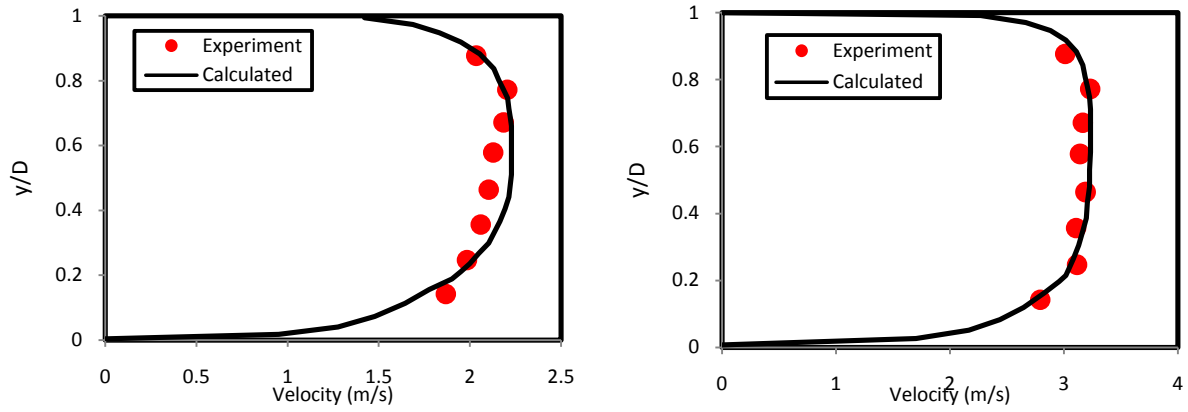

V_m=2m/s and C_v=10% V_m=3m/s and C_v=10%

Fig. 6 Vertical velocity profile for flow of 0.2mm sand particle at differentconcentration and flow velocity

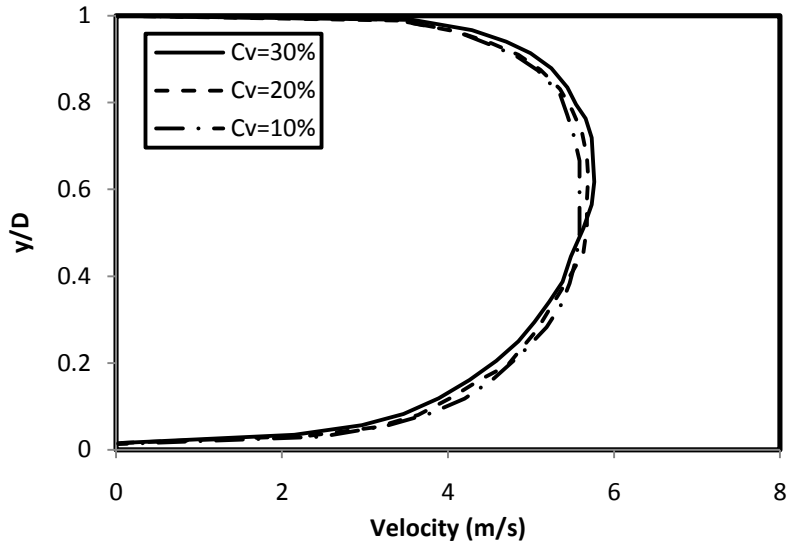

Fig. 7 Vertical velocity profile for flow of 0.2mm particle at velocity V_m=5m/s and different concentrations

5.2 Concentration Profile

Figures 8-13 show the calculated and experimental vertical concentration profiles across the pipe cross section at the pipe outlet. These figures show profiles of concentrations of solid at the pipe outlet at different particle diameter, flow velocities and efflux concentration. Data representation used in these pictures helpsunderstanding the distribution of solids across a cross sectionof the pipe. This is one of the biggest advantages of CFD, which helps to generate such type of concentration contour.

Figures 8-13show the predicted volume concentration profiles along the vertical diameter at various influx velocities, sand particle diameter and sand volume fraction. It is observed that the particles are asymmetrically distributed in the vertical plane with the degree of asymmetry increasing with increase in particle size because of the gravitational effect. It is also observed that the degree of asymmetry for the same overall concentration of slurry increases with decreasing flow velocity(Seshadri et al. [15]). This is expected, because with a decrease in flow velocity there will be a decrease in turbulent energy, which is responsible for keeping the solids in suspension.

From these figures, it is also observed that for a given velocity, increasing concentration reduces the asymmetry because of enhanced interference effect between solid particles. The effect of this interference is so strong that the asymmetry even at lower velocities is very much reduced at higher concentrations. Therefore, it can be concluded that the degree of asymmetry in the concentration profiles in the vertical plane depends upon particle size, flow velocity and overall concentration of

slurry(Kaushal et al. [7] and [12]). There are agreement between experimental and calculated concentration distributions especially or fine slurries.

Simulated concentration profiles show a distinct change in the shape for slurries of coarser particle size (i.e., 1.4 mm) with relatively high concentrations at lower velocities. It is observed that the maximum concentration at the bottom does not change and extends up to the center of the pipeline, thus making a sudden drop in the concentration in the upper half of the pipeline. The reason for such a distinct change in shape of concentration profiles may be attributed to the sliding bed/moving bed regime for coarser particles at lower velocities and higher concentrations**.**

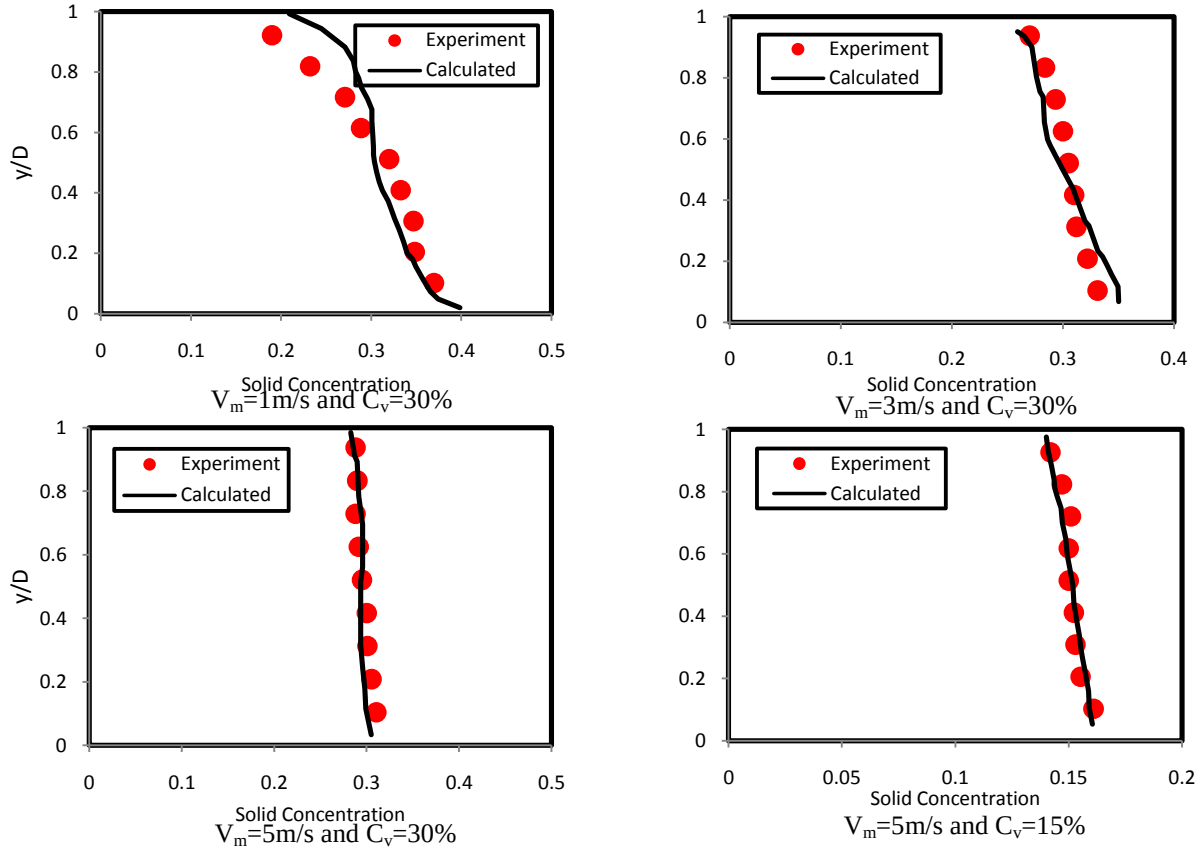

Fig. 8Vertical volume fraction profile for flow of 0.2mm particle at differentconcentrations and velocity

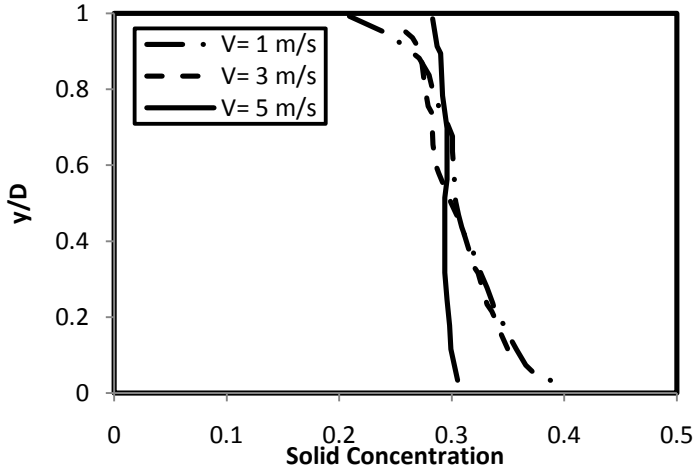

Fig. 9Concentration profiles for slurry of 0.2 mm particle size at different velocities and C_v=30%

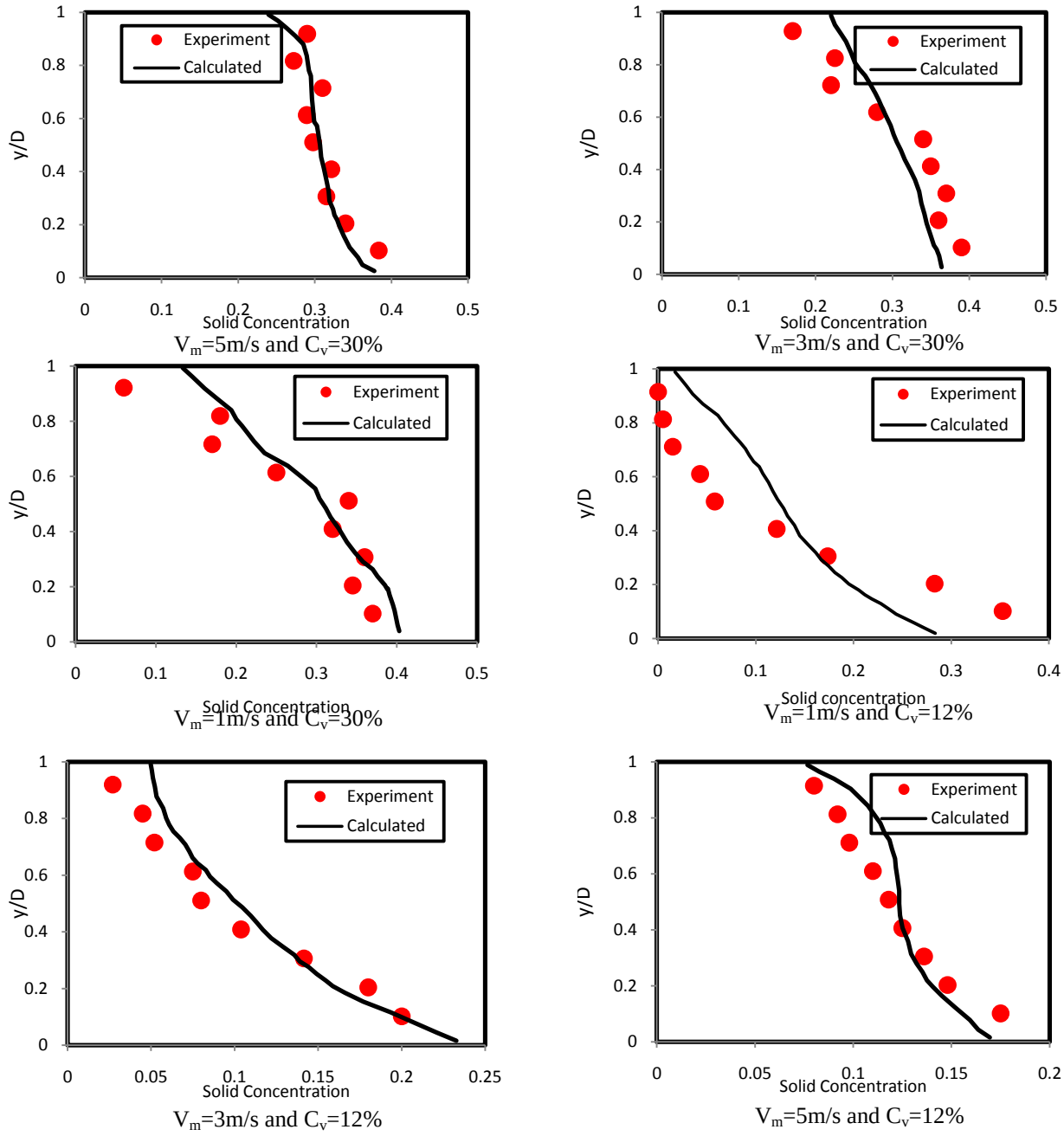

Fig. 10Vertical volume fraction profile for flow of 0.7mm particle at differentconcentrations and velocity

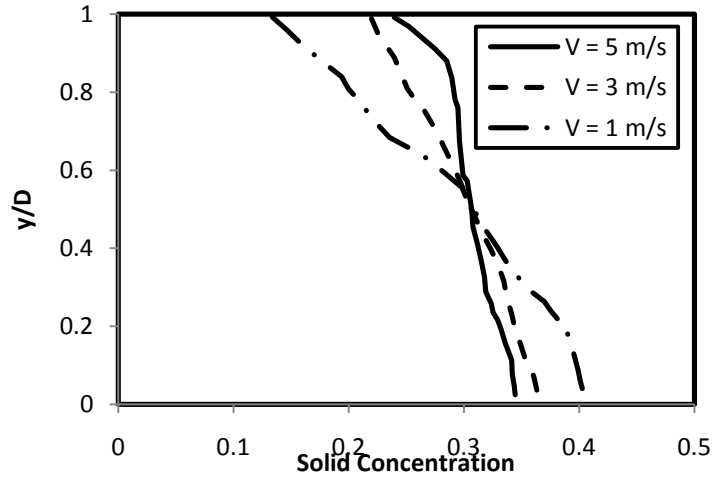

Fig. 11 Concentration profiles for slurry of 0.7 mm particle size at different velocities and C_v=30%

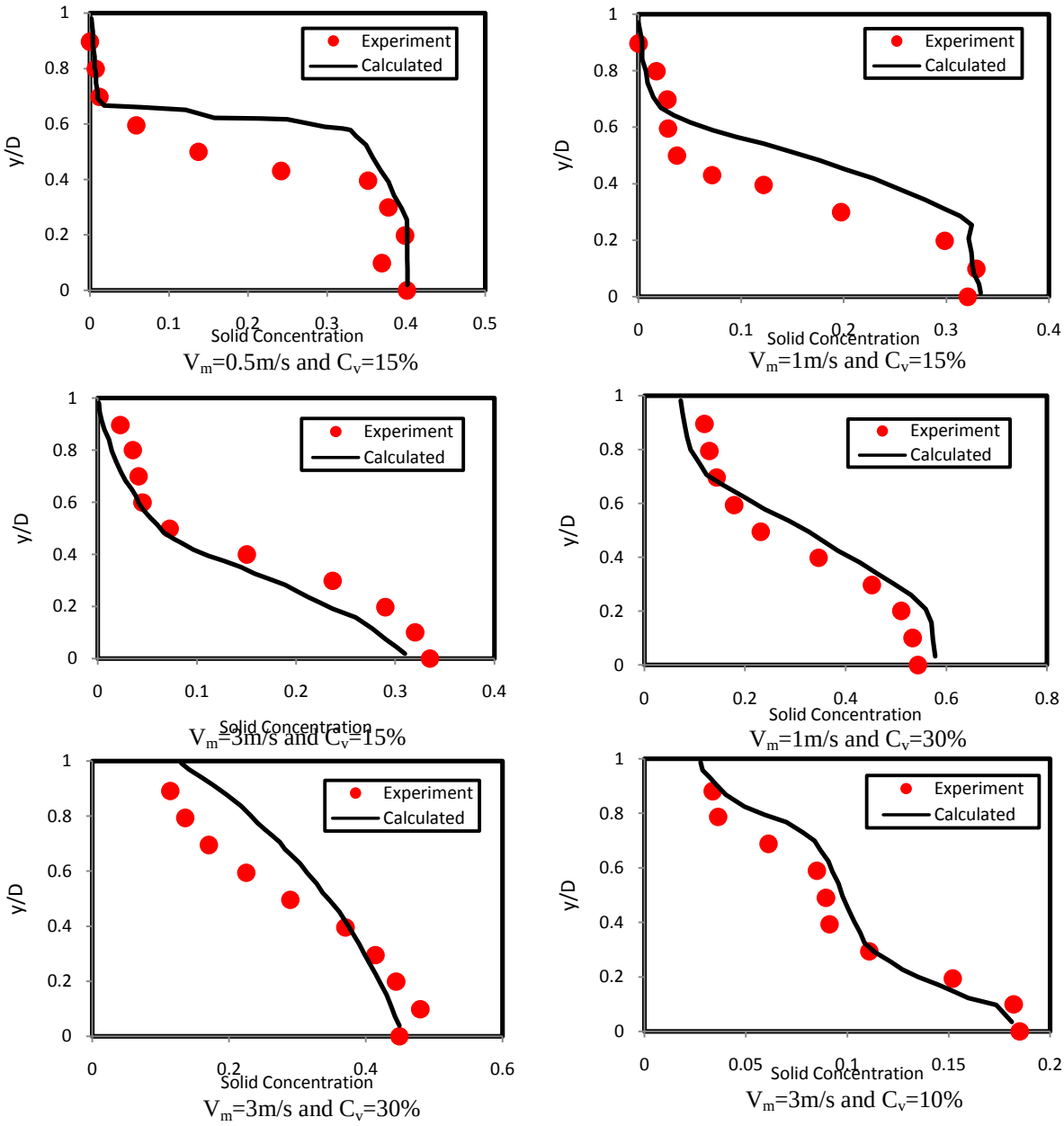

Fig. 12 Vertical volume fraction profile for flow of 1.4mm particle at differentconcentrations and velocity

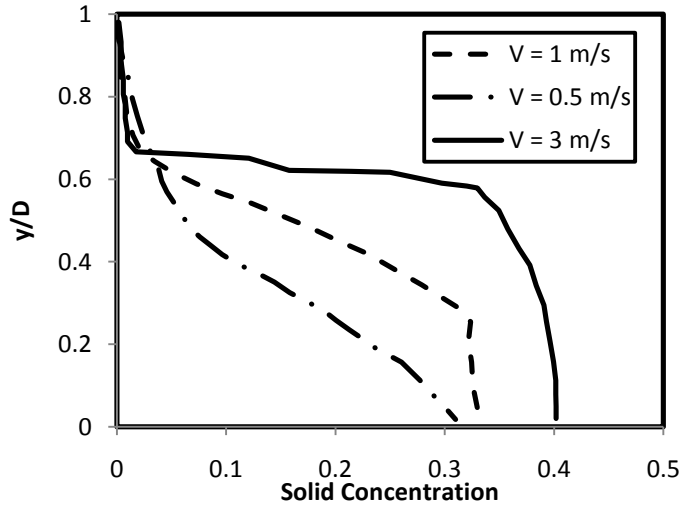

Fig. 13 Concentration profiles for slurry of 1.4 mm particle size at different velocities and C_v=15%

Due to the difference in solid concentration across the pipe diameter the drag coefficient and the settling velocity arenot constant throughout the pipe cross section and they vary along with the concentration. This non uniform distribution of drag coefficient and settling velocity give rise to different solid liquid exchange coefficients across pipe cross section. The simulation model could not capture these variations so there are some variations of the experimental results and the calculated concentration profiles that appear to be non-smooth.

5.3 Pressure drop

The aim of this study is to validate the calculated results from the simulation of the effect of the solids particle size, slurry velocity and solid concentration on the flow behavior,especially for the pressure drop of settling slurries flowing in horizontal pipes. The validation is perfumed by comparing the calculated results with the experimental results of the pressure drop.

Figures 14-16 present the effect of solid concentration, slurry mean velocity, and sand particle size on the pressure drop curves(El-Nahhas [3]). The figures show different trends in the development of pressure drop with an increase of the mean slurry velocity at different concentration, but generally the increase of the flow velocity leads to the increase in the pressure drop(Kaushal et al. [8]). The figures show also that there is a relative analogy between experimental and simulated pressure drop curves for fine slurry at all concentrations and for medium and coarse slurries at low concentrations (5% and 10%). There is a difference between experimental and simulated pressure drop curves for medium slurry and a great difference for coarse slurry at high solid concentrations (25% and 30%). Experimentally or computationally, the general trend is that increasing the solids concentration of certain slurry increases the flow pressure drop at same velocity. The rate of increase in pressure vs.concentration is small at low velocities but it increases rapidly at higher velocities. However, the curve shapes could be observed to be different for flows of solids of different sizes(Mishra et al. [11]).

In practice, the available flow area in the pipeline would be reduced, friction loss would be increased, and the pressure gradient in the slurry flow would be increased if the slurry velocity is lower than the corresponding critical deposition velocity and a stationary bed of the solids is formed in the experiments(Sundqvist et al. [13]). However, the simulation model cannot change its available flow area when the slurry flow velocity is lower than the corresponding critical deposition velocity. However, the discrepancy found between the experimental results and the calculated results in case of high solid concentration, large particle size and low velocity indicate that the developed CFD model is not fully capable to capture the phenomena at very low velocities, where the gradient of the solid profile is more in the vertical plane.

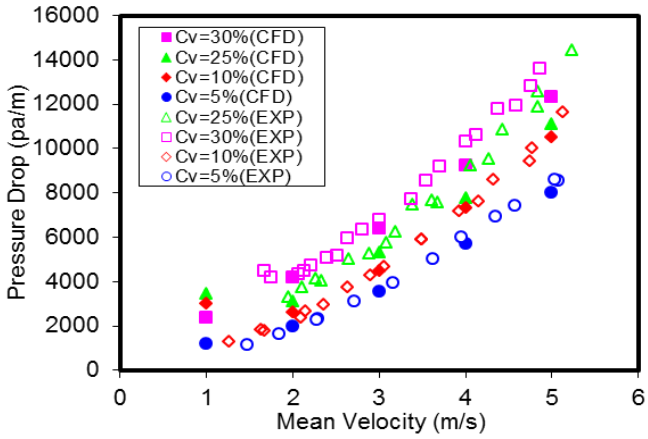

Fig. 14 Numerical pressure gradients (CFD) and experimental (EXP) for slurry of 0.2 mm particle size at different concentrations and flow velocities

5.4 Particle Size Effect

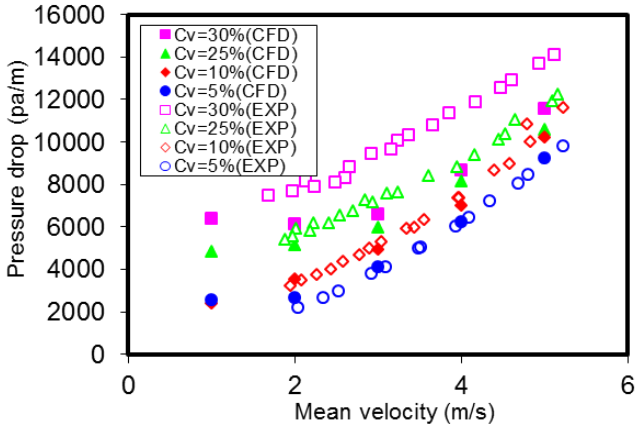

Fig. 15Numerical pressure gradients (CFD) and experimental (EXP) for slurry of 0.7 mm particle size at different concentrations and flow velocities

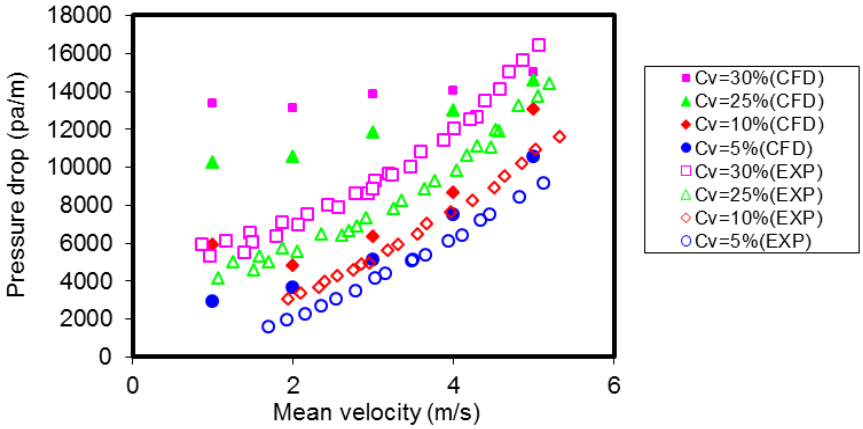

Fig. 16Numerical pressure gradients (CFD) and experimental (EXP) for slurry of 1.4 mm particle size at different concentrations and flow velocities

The variation of behavior according to the difference in solid particle size of the sand slurries could be investigated through Figures 17 and 18. These curves compare the pressure gradient of different sand particle slurries at the same solid volume fraction and velocity range. From these figures, it is observed that finer particle size has lower pressure drop than other particles at all concentrations and velocities(Gillies et al. [6]). Such an increase in pressure drop for coarser particle size especially at low velocity and high concentration is due to the increased amount of particles moving in the bed due to gravitational effect, while, in case of finer particle size, the pressure drop due to greater surface area causing more frictional losses in suspension. The coarser particles required greater power to compensate the energy loss(El-Nahhas et al. [16]). The differences between the pressure drops of different particles decrease as the slurry velocity increase. At high solid concentration (25%) fine slurry has the greatest slope of the pressure drop curves, so at ahigh slurry velocity (5m/s) it has a pressure drop greater than the medium slurry.

6. DESCRIPTION OF THREE DIMENSIONAL CFD SIMULATION

After the analysis of the results of two-dimensional simulations, new simulations were set up in three dimensions because of the axial asymmetry of the two phase flow. The purpose is to get better insight of the inherent physics of solid-liquid interaction, and to verify how the available drag coefficient models perform in three dimensions. The three dimension simulations help to visualize better the distribution of solid and liquid at the pipe outlet.

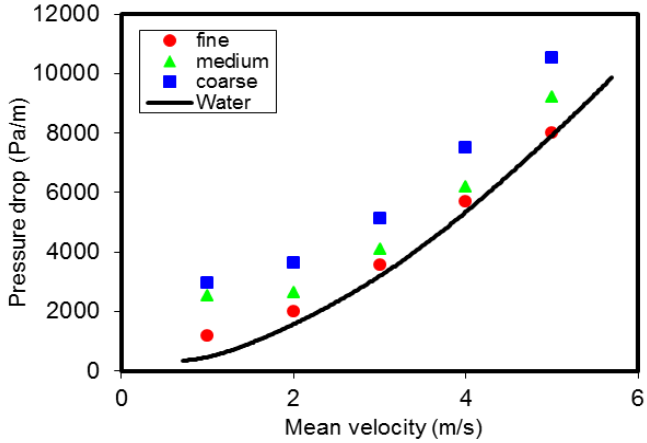

Fig. 17 Effect of solid particle size on the slurry pressure drop at C_v= 5%

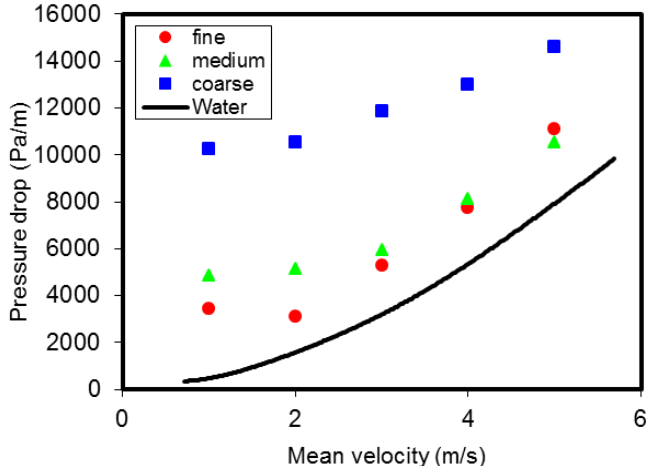

Fig. 18 Effect of solid particle size on the slurry pressure drop at C_v= 25%

Figure19 shows the distribution of the solid volume fractionat the outlet section of the pipe for a medium sand particle (d_{50}= 0.7 mm) at mean slurry velocity (V_m= 3m/s) and at solid volume fraction C_v= 15%. Looking at thefigure it's clear that the concentration at the pipe bottom has a greater value than the efflux concentration and decreased gradually upward till the minimum concentration value reached at the top of the pipe (almost water). Figure 20 shows the solid velocity distribution,where it's clear that the velocity distribution is not symmetrical about the pipe axis due to density variation. The velocity profiles in the lower half of the pipe centerline would be lower than those in the upper half(Kaushal et al. [9]).

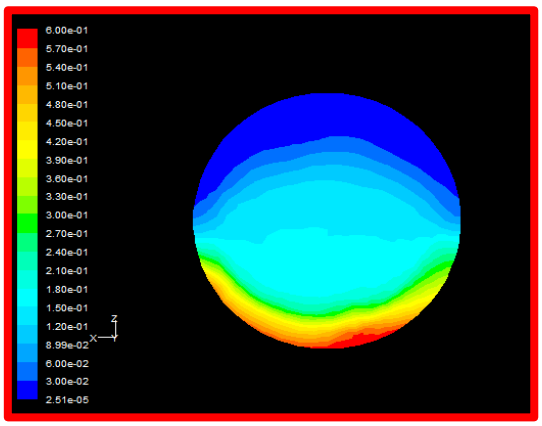

Fig. 19 Three dimensional CFD predictedvertical volumefraction profile for flow of 0.7 mm particle diameter at V_m=3m/s and C_v=15%

Due to the unavailability of experimental data, the agreement between experimental and predicted velocity and concentration profiles could not be judged. However, the profile patterns in those figures match the theoretical understanding. Therefore, it may be concluded indirectly that the CFD model is capable of validating the velocity and concentration profiles for slurry flow.

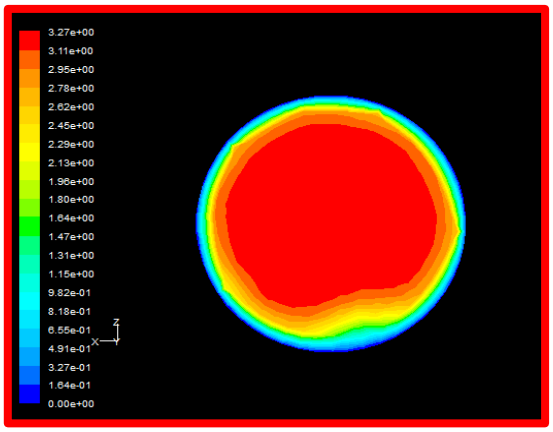

Fig. 20 Three dimensional CFD predicted vertical velocity profile for flow of 0.7 mm particle diameter at V_m=3m/s and C_v=15%

7 CONCLUSIONS

In this study, the capability of CFD was explored,in order to model complex slurry flow in pipeline. It was found that the commercial CFD softwareis capable to successfully model the slurry interactions.

1The particle concentration and velocity profiles were modeled for high concentration slurry transport where the maximum overall area-average concentration is 30% by volume employing coarse particles and high flow velocities up to 5 m/s.

2It was observed that the particles were asymmetrically distributed in the vertical plane with the degree of asymmetry increasing with increase in particle size because of the gravitational effect. It was also observed that the degree of asymmetry for the same overall concentration of slurry increased with decreasing flow velocity.

3For a given velocity, increasing concentration reduced the asymmetry because of enhanced interference effect between the solid particles. The effect of this interference was so strong that the asymmetry even at lower velocities is very much reduced at higher concentrations.

4A distinct change in the shape of concentration profiles was observed indicating the sliding bed/moving bedregimes for coarse particles at lower flow velocities.

5 The solid phase velocity profile is generally asymmetrical about the central axis at low velocity (1m/s). The asymmetry in the solid phase velocity profile is a result of particle settling due to the density difference between the two phases. The asymmetrical nature of velocity profile is reduced at higher velocity range (3-5m/s) and lower particle size.

6The increase of concentration at same slurry velocity results in the asymmetrical nature of velocity profile increases and the maximum velocity location moves more towards the top of the pipe. This effect is shown apparently for medium slurry and relatively for coarse slurry but for fine slurry the velocity profile does not change much due to increase in concentration from 10% to 30%.

7Pressure drop at any given flow velocity increases with increase in concentration and at any given concentration increases with increase in flow velocity. The rate of increase in pressure with concentration is small at low velocities but it increases rapidly at higher velocities. Finer particle size has less pressure drop than coarser particles at all concentrations and velocities.

8 There is an agreement between experimental and simulated pressure drop curves for fine slurry at all concentrations and for medium and coarse slurries at low concentrations (5% and 10%). A relative

difference for medium slurry and a great difference for coarse slurry at high solid concentrations (25% and 30%) are found.

9 Due to the axial asymmetry of the two phase flow the three dimension simulations are performed to help better visualization about the distribution of solid and liquid. The three dimension simulations give results of velocity and concentration profiles matching with two dimension simulation.

NOMENCLATURE

$C_{fr,ls}$	Coefficient of friction between l^{th} and s^{th} solid phases	[-]
$C_{1\varepsilon}$	Constant=1.44	[-]
$C_{2\varepsilon}$	Constant=1.92	[-]
C_{μ}	Constant=0.09	[-]
d_l (d_s)	Diameter of the particles	[m]
e_{ls}	Coefficient of restitution	[-]
e_{ss}	Coefficient of restitution	[-]
F_q	External body force per unit mass	[m/s^2]
$F_{lift,q}$	Lift force per unit mass	[m/s^2]
$F_{Vm,q}$	Virtual mass force per unit mass	[m/s^2]
$G_{k,m}$	Production of turbulent kinetic energy	[$kg/m.s^3$]
$g_{o,ls}$	Radial distribution coefficient	[-]
$g_{o,ss}$	Radial distribution coefficient	[-]
I_{2D}	Second invariant of the deviatoric strain rate tensor	[$1/s^2$]
K_{ls}	Inter-phase exchange drag coefficient	[$kg/m^3.s$]
K_{pq}	Inter-phase exchange drag coefficient	[$kg/m^3.s$]
N	Total number of phases	[-]
p	Pressure shared by all phases	[$kg/m.s^2$]
p_s	S^{th} solid Pressure	[$kg/m.s^2$]
v_{pq}	Interphase velocity	[m/s]
$\overrightarrow{v_m}$	Mixture velocity	[m/s]

Greek Symbols

α	Volume fraction	[-]
τ_q	q^{th} phase viscous stress tensor	[$kg/m.s^2$]
τ_s	Particulate relaxation time	[s]
λ_q	Bulk viscosity of phase q	[kg/m.s]
Φ	Angle of internal friction	[deg]
θ_s	Granular temperature	[m^2/s^2]
μ_q	Shear viscosity of phase q	[kg/m.s]
$\mu_{s,col}$	Collision viscosity	[kg/m.s]
$\mu_{s,kin}$	Kinetic viscosity	[kg/m.s]
$\mu_{s,fr}$	Frictional viscosity	[kg/m.s]
$\mu_{t,m}$	Turbulent viscosity	[kg/m.s]
σ_k	Constant=1	[-]
σ_ε	Constant=1.3	[-]

Acknowledgements

This work was extracted from Tamer Nabil Ph.D. thesis and was supported by Prof. Imam El-Sawaf and Dr. Kamal El-Nahhas.

REFERENCES

[1] Anderson, J.D.,*Computational Fluid Dynamics, The Basic and Applications*, McGraw-Hill, New york, pp.37-82, 1995.

[2] Wilson, K. C., Addie, G. R. and Clift, R.,*Slurry Transport Using Centrifugal Pumps*, London, 1992.

[3] El-Nahhas, K.,Hydraulic Transport of Dense Fine-Grained Suspensions, Ph.D. Thesis, Faculty of Engineering at Port Said, Port Said University, Egypt, 2002.

[4] Gillies, R.G., Pipeline Flow of Coarse Particle Slurries, Ph.D. thesis, University of Saskatchewan, Saskatoon, 1993.

[5] Matousek, V., Flow Mechanism of Sand-Water Mixtures in Pipelines, Ph.D. thesis, Delft University, Netherlands, 1997.

[6] Gillies, R.G. and Shook, C.A., Modelling High Concentration Settling Slurry Flows, *The Canadian Journal of Chemical Eng.* 78, pp.709–716, 2000.

[7] Kaushal, D.R. and Tomita, Y., Solid Concentration Profiles and Pressure Drop in Pipeline Flow of MultisizedParticulate Slurries,*Int. journal of multiphase flow* 28, pp.1697-1717, 2002.

[8] Kaushal, D.R. and Tomita, Y., Comparative Study of Pressure Drop in Multisized Particulate Slurry Flow Through Pipe and Rectangular Duct, *Int. J. of Multiphase Flow*, vol. 29, 1473–1487, 2003.

[9] Kaushal, D.R., Thinglas, T., Tomita, Y., Kuchii, S. and Tsukamoto, H., CFD modeling for pipeline flow of fine particles at high concentration, *Int. J. of Multiphase Flow* 43, pp.85–100, 2012.

[10] Liangyong Chen, YufengDuan, WenhaoPu, and Changsui Zhao, CFD Simulation of Coal-Water Slurry Flowing in Horizontal Pipelines, *Korean J. Chem. Eng.*, 26(4), pp. 1144-1154, 2009.

[11] Mishra, R. and Seshadri, V., Improved Model for Prediction of Pressure Drop and Velocity Field in Multisized Particulate Slurry Flow Through Horizontal Pipes, *Powder Handling and Processing Journal* 10, pp. 279–289, 1998.

[12] Kaushal, D.R. and Tomita, Y., Concentration at the Pipe Bottom at Deposition Velocity for Transportation of Commercial Slurries Through Pipeline, *Powder Technology* 125, pp. 89–101, 2002.

[13] Sundqvist, A., Sellgren, A. and Addie, G., Slurry Pipeline Friction Losses for Coarse and High Density Products,*Powder Tech.* 89, pp. 19–28, 1996.

[14] Wilson, K.C., Sanders, R.S., Gillies R.G. and Shook C.A, Verification of the Near-Wall Model for Slurry Flow, *Powder Tech.* 197, pp. 247–253, 2010.

[15] Seshadri, V. and Malhotra, R.C., Concentration and Size Distribution of Solids in Slurry Pipeline, *Proc. 11th National Conf. on Fluid Mechanics and Fluid Power*, India, pp.110–123, 1982.

[16] El-Nahhas, K., Abu-Rayan, M. and El-Sawaf, I. A., Flow Behaviour of Coarse-Grained Settling Slurries, *Proc. 12th International Water Tech. Conference*, Alexandria, Egypt, 2008.